ACS APPLIED MATERIALS & INTERFACES

Research Article

www.acsami.org

Highly Efficient Hydrophobic Titania Ceramic Membranes for Water Desalination

Joanna Kujawa,[†] Sophie Cerneaux,*[,‡] Stanisław Koter,[†] and Wojciech Kujawski[†]

[†]Nicolaus Copernicus University, Faculty of Chemistry, 7 Gagarina Street, 87-100 Torun, Poland

[‡]Institut Européen des Membranes, ENSCM, UMR 5635, CNRS, Université Montpellier 2, Place Eugène Bataillon, F-34095 Montpellier cedex 5, France

Supporting Information

ABSTRACT: Hydrophobic titania ceramic membranes (300 kD) were prepared by grafting of $C_6F_{13}C_2H_4Si(OC_2H_5)_3$ and $C_{12}F_{25}C_2H_4Si(OC_2H_5)_3$ molecules and thus applied in membrane distillation (MD) process of NaCl solutions. Grafting efficiency and hydrophobicity were evaluated by contact angle measurement, atomic force microscopy, scanning electron microscopy, nitrogen adsorption/desorption, and liquid entry pressure measurement of water. Desalination of NaCl solutions was performed using the modified hydrophobic membranes in air gap MD (AGMD) and direct contact MD (DCMD) processes in various operating conditions. High values of NaCl retention coefficient (>99%) were reached. The permeate fluxes were in the range 231−3692 $g \cdot h^{-1} \cdot m^{-2}$, depending on applied experimental conditions. AGMD mode appeared to be more efficient showing higher fluxes and selectivity in desalination. Overall mass transfer coefficients (K) for membranes tested in AGMD were constant over the investigated temperature range. However, *K* values in DCMD increased at elevated temperature. The hydrophobic layer was also stable after 4 years of exposure to open air.

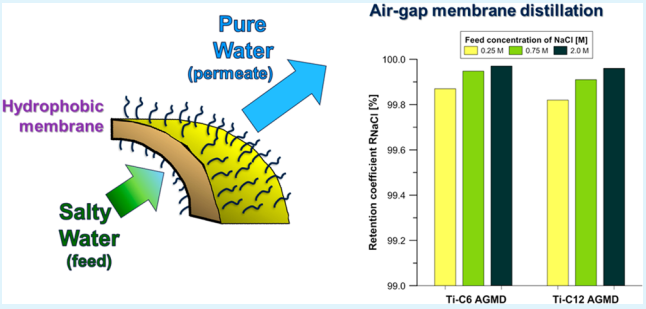

KEYWORDS: *AGMD, DCMD, desalination, hydrophobicity, perfluoroalkylsilanes*

INTRODUCTION

Membrane distillation (MD) is one of the emerging non-isothermal membrane separation processes that still needs to be improved for adequate industrial implementations.[1−6] The MD process refers to a thermally driven transport of vapors through a nonwettable porous hydrophobic membrane, with the driving force being the vapor pressure difference between the two sides of the membrane pores.[3,5,6] MD presents several significant benefits compared to other separation processes, such as multistage flash distillation (MFD), reverse osmosis (RO), nanofiltration (NF), ultrafiltration (UF), and microfiltration (MF), for example, lower operating temperatures than in distillation process and lower hydrostatic pressures than in pressure-driven processes.[1−6] In addition, high salt rejection factors are achievable, especially during treatment of water containing nonvolatile solutes.[2,7,8] Moreover, the possibility of using waste heat or alternative energy sources, such as solar and geothermal energies, enables MD to be combined with other processes into integrated systems, representing more promising separation techniques for industrial applications.[9,10]

Several MD modes, varying in the creation of the driving force can be used: direct contact membrane distillation (DCMD), air gap membrane distillation (AGMD), sweeping gas membrane distillation (SGMD), vacuum membrane distillation (VMD) and osmotic membrane distillation (OMD).[3,6,11−13] Herewith, AGMD and DCMD are discussed more in detail as both modes were applied in the present research.

In DCMD, the hot solution (feed) is in direct contact with the surface side of the membrane. Therefore, evaporation of solvent takes place at the feed-membrane interface. The vapors are transported across the membrane to the permeate side and condensed in the cold permeate inside the membrane module. Because of the hydrophobic character of the membrane, the feed cannot penetrate the membrane without applying additional pressure and therefore only the gas phase is transported within the membrane pores.

In AGMD, the hot feed solution is in a direct contact with the membrane surface, whereas on the permeate side a stagnant gas (usually air) layer exists between the membrane and the cold condensation surface located in the membrane module.[14−16] The vapors cross the air gap and condense on the cold surface inside the membrane module. The benefit of this design is thus the reduced conduction heat losses. AGMD is less versatile than DCMD because permeate is condensed on a chilled surface rather than directly in the chilled permeate.[17]

In all configurations, the liquid−vapor equilibrium is the determining factor yielding to the selectivity of the MD

Received: June 4, 2014
Accepted: August 1, 2014
Published: August 1, 2014

processes. The mass transfer in MD follows three subsequent steps: (i) liquid−vapor phase transition at the membrane pores entrance on feed side, (ii) transfer of vapors through the pores of the membrane, and (iii) condensation of vapors on the permeate side of the membrane (Figure 1).

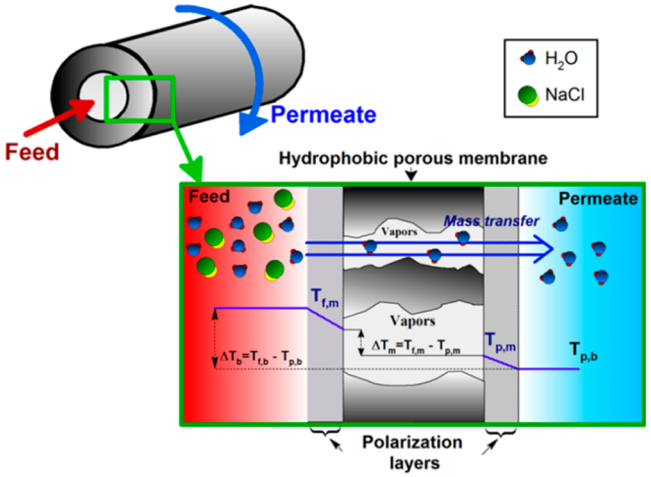

Figure 1. Mass transfer across the ceramic membrane and the temperature polarization effect occurring during the DCMD process. (T = temperature, f = feed, p = permeate, b = bulk, and m = membrane.)

According to the accepted model, the transport of solvent vapors during membrane distillation is proportional to the difference of solvent vapor partial pressure between feed and permeate.[18,19] The transport of solvent vapors can be described by eq 1.[18,19]

$$J = K(p_f - p_p) \tag{1}$$

where K = overall mass transfer coefficient [kg·m^{-2}·s^{-1}·Pa^{-1}], p_f = partial vapor pressure of water in feed, and p_p = partial vapor pressure of water in permeate.

K is an overall mass transfer coefficient, which is a reciprocal of an overall mass transfer resistance.[20] This overall resistance is a sum of three individual components (eq 2)

$$K = \left[\frac{1}{K_f} + \frac{1}{K_m} + \frac{1}{K_p}\right]^{-1} \tag{2}$$

where K_f = mass transfer coefficient of feed layer, K_m = mass transfer coefficient of membrane, and K_p = mass transfer coefficient of permeate layer.

The value of a mass transfer coefficient K involves the membrane properties such as porosity, tortuosity, pore size, material, and morphology of surface.[21] Although K depends on temperature and pressure, in many cases it is approximately constant over a wide range of system parameters.[21,22] The transmembrane water vapor pressure difference is the driving force for water vapors transfer. The water vapor pressure p_i at a given temperature can be calculated using an Antoine eq 3.[18,19,22] Coefficients A, B, and C found in Antoine's equation are characteristic for a particular solvent and for pure water values are as follows: A = 23.19, B = 3816.44, and C = −46.13.[22] Here, p_i is the vapor pressure of water in [Pa] and T is the temperature in [K].

$$p_i = \exp\left(A - \frac{B}{C + T}\right) \text{ with } i = \text{f, p} \tag{3}$$

The temperature polarization effect can also play an important role in the separation and can influence the transport properties in AGMD as well as in DCMD. The phenomenon of the temperature polarization causes that temperature at the membrane surface differs from the bulk temperature measured in the feed and in the distillate. This phenomenon is present even when the feed is pure water and can cause a driving force decrease during the transport (Figure 1).[18,23]

The porous membranes used in MD process are prepared from different hydrophobic materials, mostly from polymer materials, such a poly(propylene), poly(tetrafluoro ethylene), or poly(vinylidene fluoride).[24−27]

Recently, a growing interest to enlarge the application areas of commercial ceramic membranes has been observed.[18,19,28−30] However, ceramic materials originally possess a hydrophilic character because of the presence of the surface hydroxyl groups. In the membrane distillation process, a hydrophobic character of the membrane surface is required to prevent the membrane wetting. To widen the applications of the ceramic membranes for membrane distillation area, different surface modification procedures were suggested and studied.[18,19,28−30]

In comparison to polymeric membranes, ceramic membranes are less subjected to fouling and can be regenerated using more extreme membrane performance recovery methods, that may be hardly handled by polymeric membranes because of their temperature and pH resistance limitations.

Although ceramic membranes present a higher capital cost compared to polymeric membranes, they are able to reach high productivity because of their inherent hydrophilicity leading to reduced organic fouling, and their longer life spans. The ability to couple in-operando rapid back-pulsing allows for further

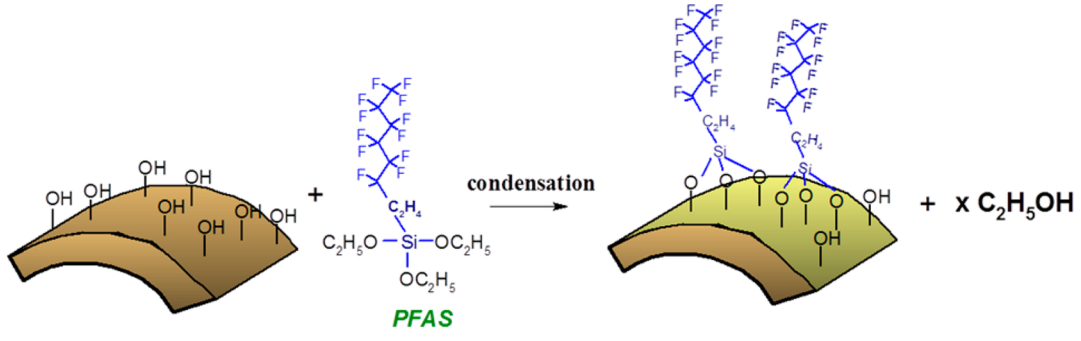

Figure 2. Scheme of surface modification of ceramic membranes by PFAS.

enhancements in operational productivity not achievable with conventional polymeric membranes.[31,32]

Surface modification of ceramic membranes can be achieved by covalently bonding the highly hydrophobic perfluoroalkoxysilane (PFAS) molecules to any available hydroxyl groups present on the oxide hydrophilic ceramic, as depicted schematically in Figure 2. The detailed discussion of the efficiency of modification is presented elsewhere.[19,28]

The main aims of presented work are focused on the modification of ceramic TiO_2 membranes and on the characterization of modified membranes in the air gap and the direct contact membrane distillation processes. Titania ceramic membranes with a molecular weight cutoff (MWCO) of 300kD (pore diameter of ca. 200 nm) were modified with two kinds of PFAS grafting molecules $C_6F_{13}C_2H_4Si(OC_2H_5)_3$ and $C_{12}F_{25}C_2H_4Si(OC_2H_5)_3$ (denoted hereafter as C6 and C12, respectively). The PFAS compounds are characterized by a different length of fluorocarbon chain. Moreover, the transport and selective properties (permeability and salt rejection rate) of modified membranes in AGMD and DCMD configurations are compared in this work. Additionally, the long-term stability of hydrophobic layer on the membrane surface was evaluated.

MATERIALS AND METHODS

Materials. TiO_2 tubular ceramic membrane (TAMI Industries, France) with MWCO of 300kD and 10/5 mm outer/inner diameters was used in present work. The samples of tubular membranes modified by C6 and C12 molecules are denoted as Ti-C6 and Ti-C12, respectively.

The 1*H*,1*H*,2*H*,2*H*-perfluorooctyltriethoxysilane (C6) and 1*H*,1*H*,2*H*,2*H*-perfluorotetradecyltriethoxysilane (C12), provided by Apollo Scientific (UK), were kept under argon atmosphere to prevent any hydrolysis and condensation reactions before their use. Chloroform stabilized by ethanol, acetone and ethanol were supplied by Carlo Erba (France). Sodium chloride was purchased from Fisher Scientific (UK). Deionized water (18 MΩ.cm) was used for the preparation of all solutions.

Grafting Process. Prior to the chemical modification, the membranes were cleaned consecutively in ethanol, acetone and distilled water for 10 min in each solvent and dried in an oven at 110 °C for approximately 12h. Preparation of C6 and C12 solutions and modification process required an inert atmosphere to avoid the polycondensation of PFAS in the presence of moisture from air. For this reason, both the preparation of grafting solutions and the modification process were performed under argon atmosphere. The modification process of ceramic membranes was performed by applying a multistep procedure described in details elsewhere.[19,28] The optimized grafting time (t_{mod}) for Ti-C6 and Ti-C12 was equal to 31.5 and 37 h, respectively.

Characterization of the Grafted Membranes. The apparent contact angle (CA) values were determined before and after ceramic membrane modification to evidence the hydrophobicity level of the modified membranes. The sessile drop method was applied to evaluate the CA values. Measurements of the static contact angles were done at room temperature using a goniometer PG-X (FibroSystem AB) for water and different concentrations of sodium chloride aqueous solutions (0.25−2 M). The contact angle measurements were performed by taking a photograph of a 4 μL liquid drop on the membrane surface and by microscope image processing (ImageJ, NIH − freeware version), with an accuracy of ±2°. The presented results are the average from 20 to 25 measurements.

Surface analysis was carried out using atomic force microscopy (AFM) equipment with a NanoScope MultiMode SPM System and NanoScope IIIa i Quadrex controller (Veeco, Digital Instrument, UK). Surface roughness was obtained from AFM images by a tip scanning.

Scanning Electron Microscope (SEM) analyses were performed using a LEO Microscope (Model 1430 Ltd., England, VP) coupled to an energy dispersive X-ray spectrometer (EDX) (Quantax 200) with a XFlash 4010 detector (Bruker AXS).

Membranes were characterized by a nitrogen adsorption/desorption analysis (ASAP 20120) using the BET equation to determine the pore size and distribution changes that might occur upon modification. Prior to the experiments the membranes were outgassed at 90 °C for 2h.

The efficiency of hydrophobization process was determined by measurements of the liquid entry pressure with water (LEPw). LEPw is defined as a pressure, at which liquid penetrates the pores and is transported through the hydrophobic membrane.[18,19,29] LEPw parameter can be therefore directly correlated with the hydrophobicity level of the modified membrane.

After the modification and determination of the LEPw values, membranes were applied in membrane distillation experiments with NaCl solutions. After each single MD experiment, the modified membrane was cleaned in pure water and dried (12 h at 110 °C) to prevent any crystallization of NaCl on the membrane surface or inside the pores.

Membrane Distillation. The membrane distillation process was performed at different conditions of feed temperature, concentration of feed solutions and mode of MD process (Table 1) utilizing grafted Ti-C6 and Ti-C12 membranes. Permeate temperature was equal to 5 °C and was constant during the whole course of the experiment.

Table 1. Conditions of Membrane Distillation Process

parameters	values
temperature of feed [°C]	70, 80, 90
temperature of permeate [°C]	5
feed concentration of NaCl [M]	0 (pure water), 0.25, 0.5, 0.75, 1.0, 2.0
MD configuration	AGMD, DCMD

NaCl solutions have been prepared using deionized water and NaCl. Salt rejection measurements have been carried out by ion chromatography (Dionex DX-100 Ion Chromatograph). The membrane distillation experiments were conducted in both AGMD and DCMD modes. Experimental rigs for AGMD and DCMD are presented schematically in Figure 3. The differences in the AGMD and DCMD setups are related to membrane modules construction and the mode of permeate collection. In the membrane module used for DCMD, the cooling solution was in a direct contact with the permeating side of the membrane, without any air gap.

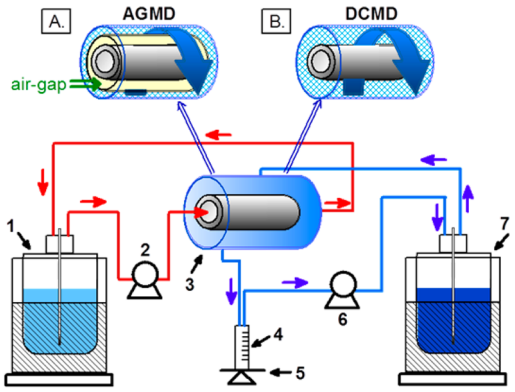

Figure 3. Scheme of the setup used in the AGMD (A) and DCMD (B) experiments (1, thermostated feed tank; 2 and 6, pump; 3, thermostated membrane module in AGMD (A) and DCMD (B); 4, measuring cylinder; 5, balance; 7, cooling system).

The permeate flux was measured by weighing the mass of liquid collected at fixed time intervals during experiments. Measurements of permeate flux were initiated after achievement of the stationary state.

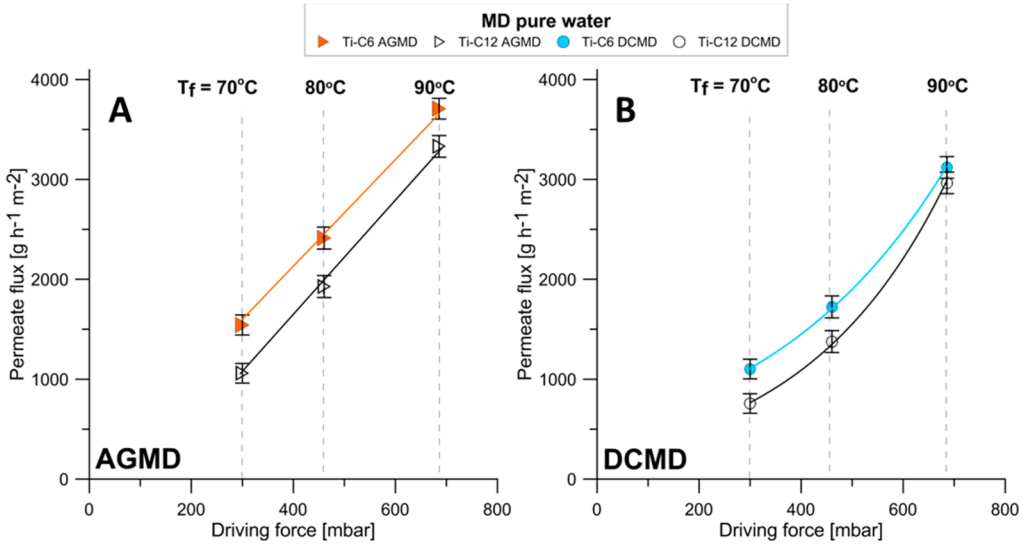

Figure 4. Permeate flux versus feed/permeate pressure difference in AGMD (A) and DCMD (B) processes of pure water. T_f = 70, 80, 90 °C; T_p = 5 °C.

The salt retention (R_{NaCl}) during the membrane distillation process was calculated according to eq 4 where C_p and C_f stand for the NaCl concentration in permeate and feed solution, respectively.

$$R_{NaCl} = \left(1 - \frac{C_p}{C_f}\right) \times 100\ [\%] \tag{4}$$

RESULTS AND DISCUSSION

Modified Membranes Characterization. Ceramic titania membranes were effectively hydrophobized since contact angle values of ~40° for both water and sodium chloride aqueous solutions increased to 135° and 145° upon modification by C6 and C12, respectively (Figure A, Supporting Information). The same values of contact angle were determined for different NaCl aqueous solutions tested.

We analyzed the probable effect of chemical modification on the roughness of the membranes by AFM. It appeared that the titania native surface was characterized by a roughness parameter Ra equal to 42 nm. Upon modification, this parameter decreased to 36 and 19 nm for C6 and C12 molecules, respectively (Figure A, Supporting Information), which represents a clear evidence of the membranes surface changes. In addition, a smoother surface was obtained for the membrane modified with the C12 molecules that have longer chains (22.1 Å) than the C6 ones (14.6 Å) and thus may cover more uniformly the surface.

According to the SEM-EDX technique, it was possible to evidence that grafting molecules were effectively present on the membrane surface as well as inside the pores. The creation of the hydrophobic thin layer covering the pores was not directly observable by scanning fractured samples. However, the presence of fluorine was easily detected by EDX (Figure A, Supporting Information).

The pore size diameters of unmodified and grafted titania membranes were measured by nitrogen adsorption/desorption. It appeared that upon modification, the pore sizes slightly decreased from 0.187 μm before grafting to 0.175 and 0.170 μm after grafting by C6 and C12 molecules, respectively (Figure B, Supporting Information). In all cases, a monomodal distribution of the pores was obtained. Moreover, we observed a strong diminution of the specific surface area (SSA) of the membranes upon grafting going from 0.78 $m^2 \cdot g^{-1}$ for the raw membrane to 0.32 and 0.17 $m^2 \cdot g^{-1}$ for C6 and C12 molecules, respectively. This behavior is in total accordance with the existence of an organic thin layer at the pore surface and is highlighted by the observation of the *C* parameter. Indeed, this constant is known to describe the interactions between the nitrogen molecules and the accessible surface since it is related to the adsorption enthalpy of the material.[33] The evident diminution of C parameter from 61 to 23 and 9 for Ti-C6 and Ti-C12, respectively is perfectly depicting the surface modification.

The various characterization techniques used confirmed the efficiency of the grafting procedure with the existence of a thin hydrophobic layer reducing slightly the size of the pores and smoothing the surface roughness.

Membrane Distillation of Pure Water. Prior to desalination experiments, membrane distillation of pure water was performed to determine the water flux through the modified titania membranes. The transport of solvent vapors in membrane distillation is proportional to the difference of water vapor pressure between the feed and the permeate (Figure 4). The driving force in membrane distillation process was calculated according to eq 3.

According to the results presented in Figure 4, it can be observed that the type of grafting molecules has an important impact on the transport properties of modified membranes. In AGMD as well as in DCMD the higher fluxes were observed for membranes grafted with C6 molecules. This behavior is related to the hydrophobicity level of modified membranes. Transport of water is higher through the less hydrophobic membrane. This phenomenon was verified by LEPw measurements. LEPw were equal to 3 bar for less hydrophobic membrane and 9 bar for membrane grafted by C12 molecules.

It can be noticed that in both MD modes, the fluxes increase with the feed temperature increase and fluxes produced in AGMD are higher than those obtained in DCMD (Figure 4). The permeate flux is increasing with the driving force value increase ($\Delta p = p_f - p_p$). However, the relation is linear only for the AGMD configuration (Figure 4). The mass transfer coefficients are constant for membranes tested in AGMD and equal to 1.46×10^{-8} and1.14×10^{-8} $kg \cdot m^{-2} \cdot s^{-1} \cdot Pa^{-1}$ for Ti-C6

dx.doi.org/10.1021/am5035297 | ACS Appl. Mater. Interfaces 2014, 6, 14223−14230

and Ti-C12, respectively. The calculated mass transfer coefficient (according to eq 2) for membranes tested in DCMD are presented in Table 2.[17,19] The overall mass transfer

Table 2. Variation of Water Vapor Overall Mass Transfer Coefficient with Feed Temperature[a]

feed temperature [°C]	overall mass transfer Ti-C6 DCMD	coefficient [kg·m^{-2}·s^{-1}·Pa^{-1}] Ti-C12 DCMD
70	1.02×10^{-8}	0.70×10^{-8}
80	1.04×10^{-8}	0.83×10^{-8}
90	1.17×10^{-8}	1.01×10^{-8}

[a] T_f = 70, 80, 90 °C; T_p = 5 °C.

coefficients K for Ti-C6 membrane in DCMD are constant at feed temperatures of 70 and 80 °C and slightly higher at 90 °C (Table 2). This fact is related to a slight or no chain mobility of fluorocarbon chains on the membrane surface. On the other hand, for C12 molecules, the overall mass transfer coefficient slightly increases at elevated temperature (Table 2). This phenomenon is associated with a higher flexibility of longer fluorocarbon chains on the modified surface. According to our estimations, the length of C6 and C12 is equal to 1.5 and 2.2 nm, respectively.

Figure 4 presents the influence of temperature on the flux of pure water. It can be seen that the permeate flux has increased exponentially with increasing temperature, so the following Arrhenius-type equation relating flux and temperature can be written (eq 5):

$$J = A \exp\left(-\frac{E_{app}}{RT}\right) \quad (5)$$

where J denotes flux, E_{app} is the apparent activation energy of the transport, R is the gas constant, and T is temperature.

It should be remembered that E_{app} is a complex quantity that includes also the influence of temperature on the driving force (i.e., vapor pressure of the feed).[34,35] The apparent activation energy (E_{app}) of the water transport was calculated for both modified membranes. According to obtained results, it can be concluded that higher values of the apparent activation energy (E_{app}) were achieved for Ti-C12 membranes (AGMD 49.2 kJ mol^{-1} and DCMD 58.8 kJ mol^{-1}) than for Ti-C6 (AGMD 43.1 kJ mol^{-1} and DCMD 56.4 kJ mol^{-1}). Moreover, marginally higher values of presented parameters were noticed during DCMD process. The obtained results were similar to data presented by Kujawski et al. (E_{app} = 51 kJ mol^{-1}).[29] Authors reported on the apparent activation energy for the water transport in pervaporation process through a hydrophobic alumina ceramic membrane modified by 1*H*,1*H*,2*H*,2*H*-perfluorodecyltriethoxysilane (C8). Such values indicate that a high energy is required to cross the potential barrier during water transport. According to presented values, it can be concluded that hydrophobicity level has a strong influence on the transport of water during separation processes.

Transport Properties of Modified Membranes in MD of NaCl Solution. This paragraph discusses the transport properties of grafted membranes in membrane distillation experiments. Figure 5 gathers the values of permeate flux through the Ti-C6 grafted ceramic membranes in AGMD (Figure 5A) and DCMD (Figure 5B) configurations.

It is seen that the permeate flux depends on the configuration mode of MD process (Figure 5). Higher values of permeate flux are observed always for AGMD mode (Figure 5A). Moreover, in both configurations, a strong influence of the feed concentration and temperature on the transport properties of modified membranes can be also noticed. The values of permeate flux through the PFAS grafted ceramic membranes are decreasing with increasing salt concentration in the feed. An increase of feed temperature results in higher fluxes due to a higher driving force.

Figure 6 shows the values of permeate flux through the Ti-C12 grafted ceramic membranes in AGMD (Figure 6A), as well as DCMD configuration (Figure 6A). Similar influence of NaCl concentration in feed solution, temperature and mode of MD process can be observed as for membranes grafted by C6 solution (Figure 5). On the other hand, an impact of the type of grafting molecules on the transport properties is also evidenced. Lower values of permeate fluxes are obtained for membranes modified by C12 molecules (Figures 5 and 6). The differences are related to the differences in the hydrophobicity level of Ti-C6 and Ti-C12 membranes.

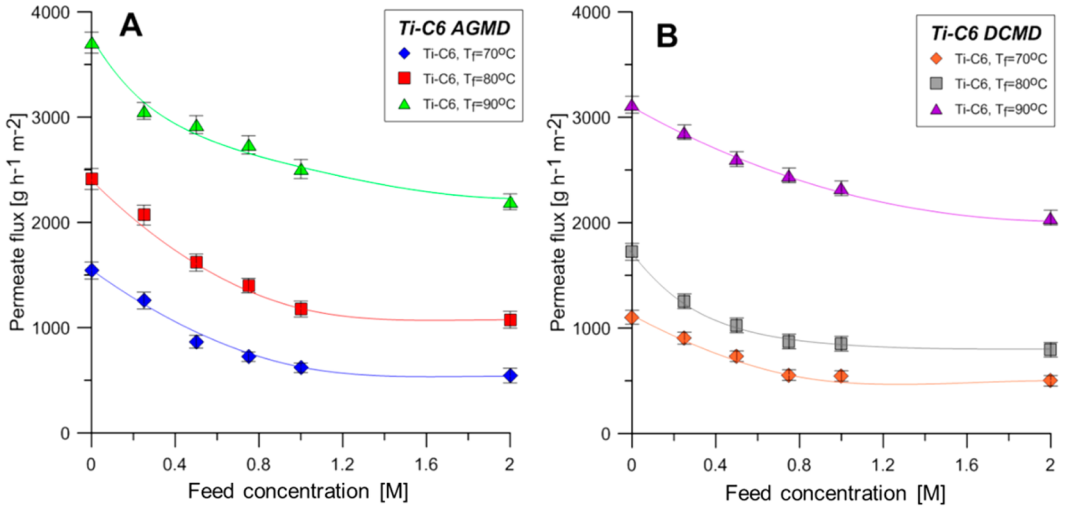

Figure 5. MD permeate flux versus NaCl concentration of the feed for the Ti-C6 grafted membrane in AGMD (A) and DCMD (B). Temperature conditions of MD: T_f = 70, 80, 90 °C; T_p = 5 °C.

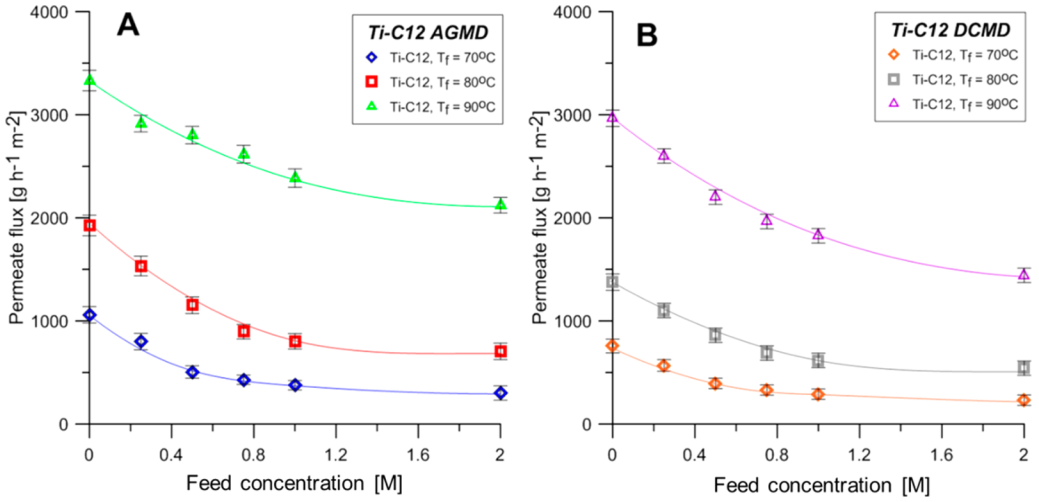

Figure 6. MD permeate flux vs NaCl concentration of the feed for the Ti-C12 grafted membrane in AGMD (A) and DCMD (B). Temperature conditions of MD: T_f = 70, 80, 90 °C; T_p = 5 °C.

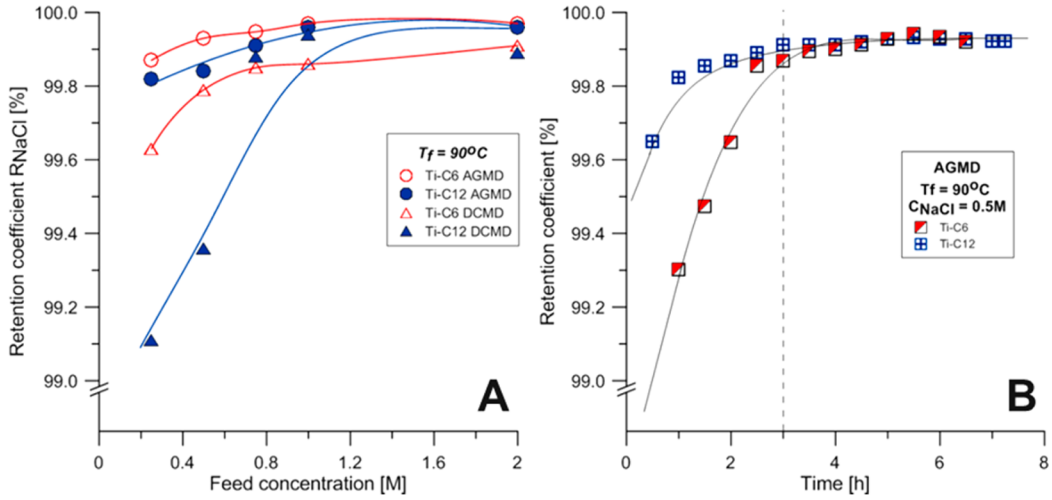

Figure 7. (A) Variation of the retention coefficient as a function of the feed concentration in desalination of NaCl solutions in DCMD and AGMD using Ti-C6 and Ti-C12. (B) Time evolution of retention coefficient of NaCl during AGMD process of 0.5 M NaCl using Ti-C6 and Ti-C12 membranes at T_f = 90 °C.

Selective Properties of Modified Membranes in MD of NaCl Solution. During transport experiments, selective properties of titania modified membranes were also evaluated in both AGMD and DCMD modes.

It can be seen that the salt retention, calculated according to eq 4, is very high (Figure 7A). These results prove (Figure 7A) that in the case of MD with aqueous solutions containing nonvolatile compounds like NaCl, practically only water vapor is transported through the membranes. As it is seen in Figure 7A, the rejection coefficient R_{NaCl} is slightly smaller than 100%. The lowest values of R_{NaCl} were observed for diluted solutions in range 0.25−0.75 M of NaCl solutions and for lower feed temperature during MD process. In addition, marginally smaller R_{NaCl} was observed for Ti-C12 membrane than for Ti-C6, comparing properties of both membranes in the same MD configuration process. In general, the lower values of R_{NaCl} were obtained in DCMD mode compared to AGMD one. Moreover, only a slight influence of feed concentration was observed for Ti-C12 in DCMD. This can be explained by the fact that some of the biggest pores could be wetted and a limited transport of NaCl solution could occur.[1] The possibility of the pore wetting was tested by measuring the retention of salt during long-lasting experiments (Figure 7B). According to the results presented in Figure 7B, it can be seen that around 3 h were needed to obtain rejection coefficient value higher than 99.8%. Despite the cleaning procedure of modified membrane after every single MD experiment, the residue sodium chloride could remain inside the pores of membranes.

Long-Term Stability of a Hydrophobic Layer. Grafted titania ceramic membranes were exposed to air for a long-time to evaluate the time of stability of hydrophobic layer. After 1.5 and 4 years, Ti-C6 and Ti-C12 membranes were used again in the AGMD experiment, applying the same conditions of feed temperature difference and feed concentration. Before both MD process, value of LEPw were also measured (Table 3). It can be concluded that long-time contact of hydrophobic layer with air had a slight impact on the LEPw values and thus on the transport properties of membranes (Table 3). The marginal decrease of LEPw, as well as permeate flux were observed for both tested membranes (Table 3). Indeed, the C6 grafted membrane tested after 1.5 years showed a permeate flux decrease of 21% against 27% for the C12 grafted membrane.

Table 3. Long-Term Stability of Surface Modified Membranes[a]

LEP_w [bar]	Ti-C6	Ti-C12
initial value of LEP_w	4	10
LEP_w value after 1.5 years storage	3	9
LEP_w value after 4 years storage	3	8
permeate flux [$g \cdot m^{-2} \cdot h^{-1}$]		
	Ti-C6	Ti-C12
initial value permeate flux	3740	3860
permeate flux value after 1.5 years storage	2930	2800
permeate flux value after 4 years storage	2540	2460
R_{NaCl} [%]		
	Ti-C6	Ti-C12
initial value of R_{NaCl}	99.9	99.8
R_{NaCl} value after 1.5 years storage	99.8	99.7
R_{NaCl} value after 4 years storage	99.8	99.6

[a]Grafting conditions: C_{C6} and C_{C12} = 0.05 M, t_{mod} = 31.5 (Ti-C6) and 37 h (Ti-C12), at room temperature. LEPw, permeate flux values and R_{NaCl} for Ti-C6 and Ti-C12 membranes. Experimental conditions: AGMD mode, feed 0.5 M NaCl, T_f = 90 °C, T_p = 5 °C.

When testing both membranes after 4 years of air exposure, we achieved permeate fluxes of around 2.5 $kg \cdot m^{-2} \cdot h^{-1}$, that corresponds to a loss of ∼34%. These results may be related to a small destruction of the hydrophobic layer on the membrane surface but also to damages generated by abrasive wear during separation process. The important point risen here is that these phenomena had no severe impact on the selective properties of the MD process since very high retention coefficients of NaCl were achieved for both membranes (Table 3). The hydrophobic layer of the ceramic titania membranes was stable after long time contact with air and maintained their hydrophobicity, yielding to R_{NaCl} values close to unity.

CONCLUSION

Titania ceramic membranes were chemically grafted by perfluoroalkylsilane molecules giving hydrophobic hybrid membranes for desalination application. The length of hydrophobic PFAS molecules has a significant impact on the hydrophobicity level of the corresponding membranes since higher LEPw value of 9 bar was reached for Ti-C12 compared to C6. However, it appeared that the highest permeate flux was obtained in both MD configurations for the Ti-C6 membrane that is characterized by a LEPw of 3 bar. This behavior was attributed to a more important pore hindrance when the longer C12 fluorocarbon chains were present within the porous membrane. Comparing the air gap and direct contact MD modes, we may conclude that the higher permeate fluxes were obtained in AGMD process whatever the membrane tested. In addition, the operating conditions in terms of feed temperatures, NaCl feed concentration and MD mode had a strong impact on the transport properties of the membranes whereas the level of hydrophobicity of tested membranes had a minimal impact on the selectivity. Slightly smaller R_{NaCl} were observed for Ti-C12 membrane than for Ti-C6 one. Generally, the retention of NaCl in both MD processes using PFAS grafted ceramic membranes is close to unity.

From a sustainable point of view, these functional ceramic membranes are stable over a long period of time of 4 years and keep their selective and transport properties in terms of desalination application. This represents a promising achievement to develop still highly performing materials and technologies to produce fresh water and an alternative technology to address the recycling of brine released from RO systems for example. In a recent review,[36] the state-of-the art related to polymer, ceramic, hybrid, and composite membranes is presented. Even though the advantages of polymers are not decried, niches applications using modified ceramics, composites and hybrid membranes are under study for their increasing potentialities that may bring new insight in seawater and brackish desalination in future. The MD process using ceramic membranes may represent a complementary technology to existing desalination solutions by treating treat brine in a multistage process coupled to RO pilots for example, since the modified membranes are also working at high feed salt concentration of 2 M.

ASSOCIATED CONTENT

Supporting Information

Characterization of unmodified and modified titania ceramic membranes by AFM, SEM-EDX techniques, CA, and pore size distribution measurements. This material is available free of charge via the Internet at http://pubs.acs.org.

AUTHOR INFORMATION

Corresponding Author

*E-mail: Sophie.Cerneaux@univ-montp2.fr. Phone: + 33467149156. Fax: + 33467149119.

Notes

The authors declare no competing financial interest.

ACKNOWLEDGMENTS

This research were supported by MNiSzW nr NN 209 255138 grant from the Polish Ministry of Science and Higher Education and 2012/07/N/ST4/00378 (Preludium 4) grant from the National Science Centre. J.K. is grateful for the Erasmus mobility grant enabling the research internship at European Membrane Institute (Montpellier, France). Special thanks are due to Ms. Karolina Jarzynka for her kind assistance with the text editing.

ABBREVIATIONS

AFM, atomic force microscopy
AGMD, air gap membrane distillation
CA, contact angle [deg]
C6, 1*H*,1*H*,2*H*,2*H*-perfluorooctyltriethoxysilane
C8, 1*H*,1*H*,2*H*,2*H*-perfluorodecyltriethoxysilane
C12, 1*H*,1*H*,2*H*,2*H*-perfluorotetradecyltriethoxysilane
C_f, concentration in feed [M]
C_p, concentration in permeate [M]
DCMD direct contact membrane distillation
J, flux [$g \cdot h^{-1} \cdot m^{-2}$]
EDX, energy dispersive X-ray spectroscopy
K, overall mass transfer coefficient [$kg \cdot m^{-2} \cdot s^{-1} \cdot Pa^{-1}$]
K_f, mass transfer coefficient of feed layer [$kg \cdot m^{-2} \cdot s^{-1} \cdot Pa^{-1}$]
K_m, mass transfer coefficient of membrane [$kg \cdot m^{-2} \cdot s^{-1} \cdot Pa^{-1}$]
K_p, mass transfer coefficient of permeate layer [$kg \cdot m^{-2} \cdot s^{-1} \cdot Pa^{-1}$]
LEPw, liquid entry pressure for water [bar]
MF, microfiltration
MFD, multistage flash distillation
MD, membrane distillation

MWCO, molecular weight cutoff
NF, nanofiltration
OMD, osmotic membrane distillation
p_f, partial vapor pressure of water in feed [mbar]
p_p, partial vapor pressure of water in permeate [mbar]
PFAS, perfluoroalkylsilane
PVA, poly(vinyl alcohol)
Ra, roughness parameter
R_{NaCl}, rejection coefficient for sodium chloride [%]
RO, reverse osmosis
SBS, styrene−butadiene−styrene
SEM, scanning electron microscopy
SGMD, sweeping gas membrane distillation
T_f, feed solution temperature [°C]
T_p, permeate solution temperature [°C]
t_{mod}, modification time [h]
Ti-C6, titania ceramic membrane grafted by C6 molecules
Ti-C12, titania ceramic membrane grafted by C12 molecules
UF, ultrafiltration
VMD, vacuum membrane distillation

REFERENCES

(1) Gryta, M.; Tomaszewska, M.; Grzechulska, J.; Morawski, A. W. Membrane Distillation of NaCl Solution Containing Natural Organic Matter. *J. Membr. Sci.* **2001**, *181*, 279−287.
(2) Smolders, K.; Franken, A. C. M. Terminology for Membrane Distillation. *Desalination* **1989**, *72*, 249−262.
(3) Betts, K. Technology Solutions: Desalination, Desalination Everywhere. *Environ. Sci. Technol.* **2004**, *38*, 246A−247A.
(4) Haggin, J. New Generation of Membranes Developed for Industrial Separations. *Chem. Eng. News* **1988**, *66*, 7−16.
(5) Pasta, M.; Wessells, C. D.; Cui, Y.; La Mantia, F. A Desalination Battery. *Nano Lett.* **2012**, *12*, 839−843.
(6) Semiat, R. Energy Issues in Desalination Processes. *Environ. Sci. Technol.* **2008**, *42*, 8193−8201.
(7) Fane, A. G.; Schofield, R. W.; Fell, C. J. D. The Efficient Use of Energy in Membrane Distillation. *Desalination* **1987**, *64*, 231−243.
(8) Liao, Y.; Wang, R.; Fane, A. G. Fabrication of Bioinspired Composite Nanofiber Membranes with Robust Superhydrophobicity for Direct Contact Membrane Distillation. *Environ. Sci. Technol.* **2014**, *48*, 6335−6341.
(9) Li, N. N.; Fane, A. G.; Ho, W. S. W.; Matsuura, T. *Advanced Membrane Technology and Applications*; John Wiley and Sons, Inc.: Hoboken, NJ, 2008.
(10) Bailey, A. F. G.; Barbe, A. M.; Hogan, P. A.; Johnson, R. A.; Sheng, J. The Effect of Ultrafiltration on the Subsequent Concentration of Grape Juice by Osmotic Distillation. *J. Membr. Sci.* **2000**, *164*, 195−204.
(11) El-Bourawi, M. S.; Ding, Z.; Ma, R.; Khayet, M. A Framework for Better Understanding Membrane Distillation Separation Process. *J. Membr. Sci.* **2006**, *285*, 4−29.
(12) Ge, Q.; Wang, P.; Wan, C.; Chung, T.-S. Polyelectrolyte-Promoted Forward Osmosis−Membrane Distillation (FO−MD) Hybrid Process for Dye Wastewater Treatment. *Environ. Sci. Technol.* **2012**, *46*, 6236−6243.
(13) Wang, P.; Chung, T.-S. A New-Generation Asymmetric Multi-Bore Hollow Fiber Membrane for Sustainable Water Production via Vacuum Membrane Distillation. *Environ. Sci. Technol.* **2013**, *47*, 6272−6278.
(14) Yao, K.; Qin, Y.; Yuan, Y.; Liu, L.; He, F.; Wu, Y. A Continuous-Effect Membrane Distillation Process Based on Hollow Fiber AGMD Module with Internal Latent-Heat Recovery. *AIChE J.* **2013**, *59*, 1278−1297.
(15) Alkhudhiri, A.; Darwish, N.; Hilal, N. Treatment of High Salinity Solutions: Application of Air Gap Membrane Distillation. *Desalination* **2012**, *287*, 55−60.
(16) Alkhudhiri, A.; Darwish, N.; Hilal, N. Produced Water Treatment: Application of Air Gap Membrane Distillation. *Desalination* **2013**, *309*, 46−51.
(17) Alklaibi, A. M.; Lior, N. Comparative Study of Direct-Contact and Air-Gap Membrane Distillation Processes. *Ind. Eng. Chem. Res.* **2006**, *46*, 584−590.
(18) Cerneaux, S.; Strużyńska, I.; Kujawski, W. M.; Persin, M.; Larbot, A. Comparison of Various Membrane Distillation Methods for Desalination Using Hydrophobic Ceramic Membranes. *J. Membr. Sci.* **2009**, *337*, 55−60.
(19) Kujawa, J.; Kujawski, W.; Koter, S.; Jarzynka, K.; Rozicka, A.; Bajda, K.; Cerneaux, S.; Persin, M.; Larbot, A. Membrane Distillation Properties of TiO_2 Ceramic Membranes Modified by Perfluoroalkylsilanes. *Desalin. Water Treat.* **2013**, *51*, 1352−1361.
(20) Guijt, C. M.; Meindersma, G. W.; Reith, T.; Haan, A. B. D. Air Gap Membrane Distillation: 2. Model Validation and Hollow Fibre Module Performance Analysis. *Sep. Purif. Technol.* **2005**, *43*, 245−255.
(21) Alklaibi, A. M.; Lior, N. Transport Analysis of Air-Gap Membrane Distillation. *J. Membr. Sci.* **2005**, *255*, 239−253.
(22) Khayet, M. Membranes and Theoretical Modeling of Membrane Distillation: A Review. *Adv. Colloid Interface Sci.* **2011**, *164*, 56−88.
(23) Sakai, K.; Koyano, T.; Muroi, T.; Tamura, M. Effects of Temperature and Concentration Polarization on Water Vapour Permeability for Blood in Membrane Distillation. *Chem. Eng. J.* **1988**, *38*, B33−B39.
(24) Martínez, L.; Florido-Díaz, F. J.; Hernández, A.; Prádanos, P. Characterisation of Three Hydrophobic Porous Membranes Used in Membrane Distillation: Modelling and Evaluation of Their Water Vapour Permeabilities. *J. Membr. Sci.* **2002**, *203*, 15−27.
(25) Essalhi, M.; Khayet, M. Self-Sustained Webs of Polyvinylidene Fluoride Electrospun Nano-Fibers: Effects of Polymer Concentration and Desalination by Direct Contact Membrane Distillation. *J. Membr. Sci.* **2014**, *454*, 133−143.
(26) Lalia, B. S.; Guillen-Burrieza, E.; Arafat, H. A.; Hashaikeh, R. Fabrication and Characterization of Polyvinylidenefluoride-*co*-Hexafluoropropylene (PVDF-HFP) Electrospun Membranes for Direct Contact Membrane Distillation. *J. Membr. Sci.* **2013**, *428*, 104−115.
(27) Tijing, L. D.; Choi, J.-S.; Lee, S.; Kim, S.-H.; Shon, H. K. Recent Progress of Membrane Distillation Using Electrospun Nanofibrous Membrane. *J. Membr. Sci.* **2014**, *453*, 435−462.
(28) Kujawa, J.; Kujawski, W.; Koter, S.; Rozicka, A.; Cerneaux, S.; Persin, M.; Larbot, A. Efficiency of Grafting of Al_2O_3, TiO_2 and ZrO_2 Powders by Perfluoroalkylsilanes. *Colloids Surf., A* **2013**, *420*, 64−73.
(29) Kujawski, W.; Krajewska, S.; Kujawski, M.; Gazagnes, L.; Larbot, A.; Persin, M. Pervaporation Properties of Fluoroalkylsilane (FAS) Grafted Ceramic Membranes. *Desalination* **2007**, *205*, 75−86.
(30) Larbot, A.; Gazagnes, L.; Krajewski, S.; Bukowska, M.; Wojciech, K. Water Desalination Using Ceramic Membrane Distillation. *Desalination* **2004**, *168*, 367−372.
(31) Lee, S.; Cho, J. Comparison of Ceramic and Polymeric Membranes for Natural Organic Matter (NOM) Removal. *Desalination* **2004**, *160*, 223−232.
(32) Kim, J.; Van der Bruggen, B. The Use of Nanoparticles in Polymeric and Ceramic Membrane Structures: Review of Manufacturing Procedures and Performance Improvement for Water Treatment. *Environ. Pollut.* **2010**, *158*, 2335−2349.
(33) Guerrero, G.; Mutin, P. H.; Vioux, A. Anchoring of Phosphonate and Phosphinate Coupling Molecules on Titania Particles. *Chem. Mater.* **2001**, *13*, 4367−4373.
(34) Song, K.-H.; Lee, K.-R. Pervaporation of Flavors with Hydrophobic Membrane. *Korean J. Chem. Eng.* **2005**, *22*, 735−739.
(35) Xianshe, F.; Huang, R. Y. M. Estimation of Activation Energy for Permeation in Pervaporation Processes. *J. Membr. Sci.* **1996**, *118*, 127−131.
(36) Camacho, L. M.; Dumée, L.; Zhang, J.; Li, J.; Duke, M.; Gomez, J.; Gray, S. Advances in Membrane Distillation for Water Desalination and Purification Applications. *Water* **2013**, *5*, 94−196, DOI: 10.3390/w5010094.